

Analyst

Accepted Manuscript



This is an *Accepted Manuscript*, which has been through the Royal Society of Chemistry peer review process and has been accepted for publication.

Accepted Manuscripts are published online shortly after acceptance, before technical editing, formatting and proof reading. Using this free service, authors can make their results available to the community, in citable form, before we publish the edited article. We will replace this *Accepted Manuscript* with the edited and formatted *Advance Article* as soon as it is available.

You can find more information about *Accepted Manuscripts* in the [Information for Authors](#).

Please note that technical editing may introduce minor changes to the text and/or graphics, which may alter content. The journal's standard [Terms & Conditions](#) and the [Ethical guidelines](#) still apply. In no event shall the Royal Society of Chemistry be held responsible for any errors or omissions in this *Accepted Manuscript* or any consequences arising from the use of any information it contains.

1
2
3 **Quality Assessment of Recombinant Proteins by Infrared Spectroscopy.**
4 **Characterisation of a Protein Aggregation Related Band of the Ca²⁺-**
5 **ATPase**
6

7
8 **Chenge Li¹, Cédric Montigny^{2,3,4}, Marc le Maire^{2,3,4}, Andreas Barth^{1*}**
9 Department of Biochemistry and Biophysics, Stockholm University, Sweden
10

11 ¹ Department of Biochemistry and Biophysics, Stockholm University, Sweden,

12 ² CEA, iBiTec-S, Saclay, France,

13 ³ CNRS, UMR 8221, France,

14 ⁴ Université Paris-Sud, France.

15
16 *Corresponding author. A Barth, Department of Biochemistry and Biophysics, Arrhenius
17 Laboratories, Stockholm University, SE-106 91 Stockholm, Sweden. Tel.: +46 8 162452;
18 Fax: +46 8 155597; E-mail: Andreas.Barth@dbb.su.se
19

20
21
22 **Abstract**
23

24 Infrared spectroscopy was used to characterise recombinant sarcoplasmic reticulum Ca²⁺-
25 ATPase (SERCA1a). In the amide I region, its spectrum differed from that of Ca²⁺-ATPase
26 prepared from rabbit fast twitch muscle below 1650 cm⁻¹. A band at 1642 cm⁻¹ is reduced in
27 the spectrum of the recombinant protein and a band at 1631 cm⁻¹ is more prominent. By
28 comparison of amide I band areas with the known secondary structure content of the protein,
29 we assigned the 1642 cm⁻¹ band to β -sheet structure. Further investigation revealed that the
30 1642 cm⁻¹ band decreased and the 1631 cm⁻¹ band increased upon storage at room
31 temperature and upon repeated washing of a protein film with water. Also protein aggregates
32 obtained after solubilisation of the rabbit muscle enzyme showed a prominent band at 1631
33 cm⁻¹, whereas the spectrum of solubilised ATPase resembled that of the membrane bound
34 protein. The spectral position of the 1631 cm⁻¹ band is similar to that of a band observed for
35 inclusion bodies of other proteins. The findings show that the absence of the 1642 cm⁻¹ band
36 and the presence of a prominent band at 1631 cm⁻¹ indicate protein aggregation and can be
37 used as a quality marker for the optimisation of recombinant protein production. We conclude
38 that recombinant production of SERCA1a, storage at room temperature, repeated washing and
39 aggregation after solubilisation all modify existing β -sheets in the cytosolic domains so that
40 they become similar to those found in inclusion bodies of other proteins.
41
42

43
44
45 *Keywords:* Amide I absorption, Ca²⁺-ATPase, Enzyme activity, FTIR spectroscopy, Inclusion
46 body, Infrared spectroscopy, P-type ATPase, Protein aggregation, Recombinant proteins,
47 Secondary structure
48

49 *Abbreviations:* ATP, adenosine-5'-triphosphate; ATR, attenuated total reflection; FTIR,
50 Fourier transform infrared; IR, infrared; SERCA1a, sarco-endoplasmic reticulum Ca²⁺-
51 ATPase isoform 1a; SR, sarcoplasmic reticulum
52
53
54
55
56
57
58
59
60

1. Introduction

Infrared (IR) spectroscopy is a useful technique in many areas, such as identification of unknown compounds, quality control, and scanning the effects of changing conditions like temperature and pH on the molecule of interest. The application of IR spectroscopy to the study of protein structure can be traced back to the 1950s,¹ and now it is a well-established tool for protein structure analysis²⁻⁴. The sensitivity of IR spectroscopy to molecular conformation makes it valuable for protein secondary structure analysis. The assignment of secondary structures has been achieved by both theoretical calculation and experimental observation of proteins that are rich in a certain secondary structure. Thus IR spectroscopy has been successfully applied to investigate structure and stability of recombinant proteins⁵⁻¹⁰. Here, we apply the method to assess the structural integrity of recombinant Ca²⁺-ATPase.

Sarco-endoplasmic reticulum Ca²⁺-ATPase isoform 1a (SERCA1a) is the major membrane protein in the sarcoplasmic reticulum (SR) with a molecular weight about 110 kDa¹¹. It pumps calcium from the cytosol back to the SR lumen during muscle relaxation, driven by the energy of adenosine-5'-triphosphate (ATP) hydrolysis.^{12, 13} In its catalytic cycle, the transport sites change their orientation and affinity for Ca²⁺. They have higher Ca²⁺ affinity and are accessible from the cytoplasmic side in the E1 state. Two Ca²⁺ bind to the E1 form (Ca₂E1). Subsequently, the enzyme gets phosphorylated by ATP (Ca₂E1P) which is followed by a conformational change to a low Ca²⁺ affinity form (E2P). As a consequence, Ca²⁺ is released to the luminal side of the membrane. The cycle ends with dephosphorylation and a return to the E1 state. Crystal structures show that the enzyme undergoes large structural changes in both the cytoplasmic portion and the transmembrane region.¹³⁻¹⁷

IR spectroscopic studies of the structure and the mechanism of SERCA1a have been carried out by several groups^{3, 18-26}. Still, and in spite of the detailed structural knowledge obtained by X-ray crystallography, several questions regarding the molecular mechanism have not yet been answered. They include (i) the mechanism of proton countertransport and the identity of the residues that become protonated when Ca²⁺ leaves its binding sites, (ii) the effect of mutations associated with diseases like Brody disease, and (iii) the mechanism of coupling between the phosphorylation site and the Ca²⁺ binding sites which are 50 Å apart. This coupling implies long-range communication between these sites for efficient transport via conformational changes. Current explanations of conformational change combine elements of the "induced fit" and the "conformational selection" models: binding or chemical modification generates local strain, which leads to propagation of the structural perturbation through the protein via pre-existing conformations until the strain is dissipated and a new main conformation is reached²⁷. For the Ca²⁺-ATPase, these propagation pathways need now to be identified. One way of addressing these open questions is the study of the effects of point mutations on structure and function of the enzyme, which requires recombinant production of the enzyme. However, before the role of individual amino acids for the catalytic mechanism can be studied, the quality of the recombinant enzyme has to be thoroughly tested. Recently we have shown that the active fraction of recombinant wild type SERCA1a produced and purified from *Saccharomyces cerevisiae* behaves as native SERCA1a regarding the enzymatic activity and the conformational changes during the reaction cycle²⁸. As we report in this work however, the IR absorption spectrum in the amide I region, sensitive to secondary structure, was slightly different regarding bands at 1642 and 1631 cm⁻¹. The debated assignment of the 1642 cm⁻¹ band makes it interesting to investigate the nature of this band further. We find that the differences between native and recombinant protein can be explained by partial aggregation of the latter leading to β-sheet structures which are similar to those in inclusion bodies of other proteins. The implications of this work extend to other recombinant proteins also, as the findings imply a simple quality control for the protein product.

2. Materials and Methods

2.1 Sample preparation

Rabbit SERCA1a at 10 mg.mL⁻¹ was a generous gift from W. Hasselbach (Max-Planck-Institut, Heidelberg, Germany) and prepared as described previously²⁹. Recombinant SERCA1a at 3 mg.mL⁻¹ was prepared in a yeast based expression^{28, 30-32}. The enzyme was expressed with a biotin acceptor domain linked to the C-terminus via a thrombin cleavage site, and purified in a single step with avidin affinity chromatography. The enzyme was initially solubilised in *N*-dodecyl- β -maltopyranoside (DDM, Affymetrix), then reconstituted into phospholipids (egg-yolk phosphatidylcholine/egg-yolk phosphatidic acid, w/w=9/1, Avanti Polar Lipids). The phospholipids were added at a ratio of $m_{\text{lipid}}/m_{\text{protein}}=3:1$, and DDM was removed by adding biobeads at a ratio of $m_{\text{biobeads}}/m_{\text{DDM}}=200:1$. Native and recombinant proteins were centrifuged and the supernatant was discarded to remove glycerol. The centrifugation step was performed with a TLA-55 rotor at a speed of 154000 g at 4 °C. Unless stated otherwise, the proteins were resuspended in MOPS buffer (10 mM MOPS-KOH, 10 mM KCl, 20 μ M CaCl₂, pH 7.0) to give the same protein concentrations as before centrifugation.

Solubilised SERCA1a was prepared by solubilising of rabbit SERCA1a after centrifugation in 1 mg.mL⁻¹ DDM in the above MOPS buffer with a protein/detergent (w/w) ratio 1:20. It was obtained from the supernatant after centrifugation at 154000 g for 1 hour. The pellet contained mainly aggregated protein. It was mixed with the above MOPS buffer and subsequently vortexed but did not resuspend completely.

2.2 Attenuated total reflection (ATR) measurements for the assessment of secondary structure

IR spectra were recorded at room temperature (20°C) and 4 cm⁻¹ resolution using a Bruker Vertex 70 spectrometer equipped with a SensIR 9-reflection diamond ATR accessory. 100 interferometer scans were averaged for each spectrum. IR samples were prepared in the following way: membrane bound rabbit SERCA1a was diluted 4-fold with the MOPS buffer specified above, then 4 μ L diluted membrane bound rabbit or recombinant SERCA1a, or 10 μ L solubilised rabbit protein (see 2.1) were added onto the diamond ATR crystal. In order to achieve a much higher signal to noise ratio, the sample was dried within 5 min in a gentle stream of N₂, which formed a protein/lipid film on the surface of the crystal. IR spectra were recorded during and after removal of bulk water and the progress of drying was monitored using the absorption of the OH stretching vibrations of water. The second derivative spectra recorded during the final drying phase were analysed as to whether the spectral positions of the bands changed. This would indicate a conformational change caused by drying, but was not observed. In the first spectrum analysed in this way, the absorbance of the H₂O bending vibration was significantly larger than that of the protein amide I vibration. This indicates that the sample at this stage of the drying process was more dilute than the samples that we commonly use to study the catalytic mechanism and which were demonstrated to undergo all major partial reactions in the catalytic cycle^{24, 33, 34}. Thus, no structural change was detected in the transition from a state where the ATPase is known to be fully functional to the dry film. This is in line with our observation that drying and immediate rehydration has little effect on enzyme activity³⁵. We conclude that samples prepared in this way are structurally and functionally intact.

1
2
3 In one series of experiments, the protein film on the ATR crystal was washed several times
4 to remove soluble compounds: 5 μL ddH₂O was added carefully to the film and removed after
5 5 min by placing a tissue on the side of the liquid without touching the film. The tissue was
6 removed before spectra recording. The first addition of water dissolved a small fraction of the
7 proteins. Subsequent additions did not change the protein absorption indicating that the
8 protein film was unaffected by the procedure.
9

10 11 **2.3 Reaction induced Fourier transform infrared (FTIR) difference spectroscopy for** 12 **activity measurements** 13

14
15 Enzyme activity was measured at 1°C as described previously^{28, 36}. 1 μL 10 mM dithiothreitol
16 and 2 μL 10 mM caged ATP solution were dried on a CaF₂ window with a 5 μm trough, and
17 then 2 μL SERCA1a sample in MOPS buffer (10 mM MOPS-KOH, 10 mM KCl, pH 7.0) and
18 8 μL MOPS buffer (10 mM MOPS-KOH, 10 mM KCl, 20 μM CaCl₂, pH 7.0) were dried on
19 the window and rehydrated with 1 μL 3 mM MgCl₂. IR spectra were recorded with a Bruker
20 IFS 66 FTIR spectrometer equipped with an HgCdTe detector at 4 cm^{-1} resolution. After
21 recording a reference spectrum consisting of 1000 interferometer scans, a UV flash
22 photolysed the caged ATP, which initiated the reaction cycle. Thereafter, the conformational
23 changes of the enzyme as well as the hydrolysis reaction catalysed by the enzyme were
24 followed in real time by recording time-resolved IR spectra. The number of scans per
25 spectrum increased from 1 to 10, 40 and 200 after each block of 10 spectra. The 1245 cm^{-1}
26 band, which has been assigned to the antisymmetric stretching vibration of PO₂⁻ groups³⁷,
27 indicated ATP consumption and was used for activity measurements^{28, 36}. The relative specific
28 enzyme activity in terms of reactant consumption divided by protein absorption was
29 calculated as the initial change of the 1245 cm^{-1} band relative to the protein amide II
30 absorbance.²⁸ We term this quantity the activity in spectral units. It can be converted to SI
31 units using calibrations between protein mass and amide II absorbance and between the
32 photolysis bands at 1345 and 1527 cm^{-1} and the amount of released ATP: (i) an amide II
33 absorbance of 1 is produced by 0.69 mg SR protein per cm^2 ($\pm 17\%$)^{33, 38} and (ii) photolysis
34 bands at 1345 and 1527 cm^{-1} with an absorbance of 0.001 are produced by the release of 14.6
35 and 5.2 nmol ATP per cm^2 ($\pm 8\%$), respectively³⁸.
36
37
38
39

40 41 **2.4 Curve fitting of the ATR-IR spectra** 42

43 The ATR-IR spectra were fitted in an iterative procedure using the Levenberg-Marquardt
44 algorithm as implemented in the OPUS software from our spectrometer supplier Bruker. First,
45 the band positions of the component bands were determined from the second derivative
46 spectra. Then, the absorption spectrum was fitted using these band positions as fixed
47 parameters. Each component band was represented by a mixture of a Gaussian and a
48 Lorentzian band. A broad band at 1600 cm^{-1} was included which served a similar function as
49 the baseline corrections applied by other authors. Subsequently, the second derivatives of the
50 fit and the experimental spectrum were compared by eye. While the absorption spectrum was
51 fitted very well, the second derivatives of fit and experimental spectrum showed clear
52 differences. Therefore a selection of band parameters like position, width and amplitude were
53 changed manually and fixed in the fit and additional bands added. The fit to the absorption
54 spectrum was repeated with the new parameters and the second derivatives of fit and
55 experimental spectrum again compared by eye. This procedure was repeated until a
56 satisfactory agreement between fit and experimental spectrum was obtained for both, the
57 absorption spectrum and the second derivative spectrum.
58
59
60

3. Results

3.1 Assessment of secondary structure - ATR measurements on rabbit and recombinant SERCA1a

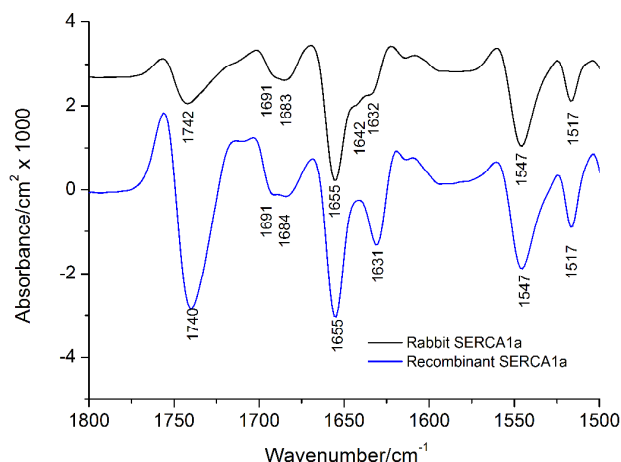


Fig. 1 Secondary structure analysis of rabbit (black) and recombinant SERCA1a (blue). Shown are the second derivatives of the ATR infrared spectra of protein films.

We analysed the secondary structure of rabbit and recombinant ATPase using the second derivative of ATR-IR spectra shown in Fig. 1. Second derivatives were calculated to enhance the apparent resolution of the absorption spectra. Negative bands in the second derivative spectrum show component bands that are often difficult to see in the absorption spectrum.

In the spectrum of SERCA1a protein films, there are 4 main absorption bands between 1800 and 1500 cm^{-1} , the lipid C=O band (1760-1700 cm^{-1}), the amide I band, which is sensitive to secondary structure (1700-1610 cm^{-1}), the amide II band (1535-1565 cm^{-1}), and the C-C stretching band of the tyrosine ring (~ 1517 cm^{-1}). In the lipid C=O region, rabbit SERCA has a band at 1742 cm^{-1} and the recombinant protein a band at 1740 cm^{-1} . The amplitude of this band is larger for the recombinant protein, indicating a higher lipid/protein ratio, which is favourable for maintaining enzyme activity³⁹. Its spectral position is slightly different for the two preparations, which could be due to the different lipid composition of the membranes and/or the different protein content.

In the amide I region, 5 main amide I component bands were observed in the second derivative of the absorbance spectrum for rabbit SERCA1a and they are found at 1691, 1683, 1655, 1642 and 1632 cm^{-1} (Fig. 1). These band components have been described previously and our spectra compare favourably with the previous work^{18, 20-22, 40}. A more direct comparison is difficult, because the previous studies often used samples in D_2O , different spectral resolutions, and analysed the amide I band mostly using Fourier self-deconvolution with different parameters. However, evaluating our data with fine-structure enhancement, which produces very similar spectra as Fourier self-deconvolution⁴¹, generates resolution enhanced spectra that are very similar to previous work in H_2O solution²⁰ regarding spectral shape, component band position, and relative component band intensity (not shown). The band at 1655 cm^{-1} is due to α -helix and irregular structures, the bands at 1691 and 1684 cm^{-1} are mainly attributable to β -sheet and turn structures, and the band at 1632 cm^{-1} has been assigned to β -sheet structures^{18, 20-22, 40}. The 1642 cm^{-1} band has also been described previously but so far there is no clear assignment for this band. It was suggested to arise from

α -helix^{18, 20}, or from irregular structure^{21, 40}.

The recombinant protein showed similar band positions as rabbit SERCA1a in the amide I region, except that the bands at 1642 and 1632 cm⁻¹ were replaced by a single band at 1631 cm⁻¹ indicating different structures. These differences were also observed in transmission experiments where the samples were in aqueous solution (not shown). The difference between rabbit SERCA1a and recombinant protein made it interesting to investigate the nature of the 1642 cm⁻¹ band and the reason behind the different structures. These experiments, described in the following sections, were done on the rabbit SERCA1a sample.

3.2 Band assignment for the 1642 cm⁻¹ band

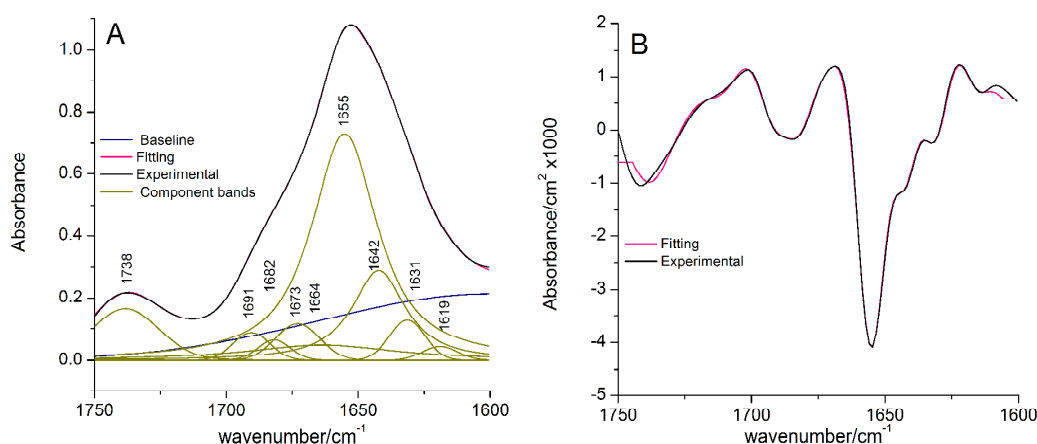


Fig. 2 Curve fitting analysis of the ATR IR spectrum of a freshly prepared dry film of membranous rabbit SERCA1. A: absorption spectrum, B: second derivative spectrum. In most spectral regions, fit and experimental spectrum superimpose so well that the fit cannot be discerned.

In the following, the interpretation of the amide I component bands is guided by the known secondary structure content from X-ray crystallography^{1, 42-49}. Here we use this approach to assign the 1642 cm⁻¹ band. As a starting point, curve fitting was used to quantify the contributions of the overlapping bands in the amide I region. The aim was to get the best fit for both the absorption spectrum as well as the second derivative spectrum. The experimental spectra (black) and the fits (pink) are shown in Fig. 2. They overlap so well that the fit is hidden behind the experimental curve in most spectral regions. In the 1750-1600 cm⁻¹ region, ten bands were used to fit the absorption spectrum. One of them was positioned at 1600 cm⁻¹ and served as baseline (blue curve in Fig. 2). From the remaining 9 bands (olive curves in Fig. 2), 7 bands were located in the amide I region and their relative band areas are listed in Table 1. 6 of these bands have been used previously at similar spectral positions to fit the ATPase spectrum obtained in H₂O^{20, 25}. The difference is that our model has 4 bands above 1660 cm⁻¹ where the previous models have 3 bands. Two of these bands were introduced in our model to improve the agreement between the second derivatives of the fit and of the experimental spectrum. The combined relative area of these bands is 18% in our case, ~20%²⁵ and 31.5%²⁰ in the previous work. The contribution of the band of α -helices and unordered structures at 1655 cm⁻¹ has in our model a significantly larger contribution (59%) than in the previous work (39%²⁵ and 23.1%²⁰), but compares favorably with the helical content (47%) determined from the X-ray structure (see below), given that not only helices are expected to absorb near 1655 cm⁻¹. The 1642 cm⁻¹ band has a similar contribution (19%, 20%²⁵, 22.3%²⁰) and the 1631 cm⁻¹ band contributes considerably less in our study (4% versus 22%²⁵ and 16.3%²⁰).

To explain the discrepancies we tested the robustness of our results. Fits to the absorption spectrum with fixed band positions but otherwise free band parameters (amplitude, width, shape) could also produce fits of which the 2nd derivative was close to the experimental 2nd derivative in the 1652 to 1625 cm⁻¹ region. They also gave very similar band areas for the 1642 and 1631 cm⁻¹ bands (4-5 % and 22-24%) depending on the starting parameters. The deviations for the other band areas were larger. In particular the 1655 cm⁻¹ band area could be as low as 34%, but such fits showed deviations between the 2nd derivative spectra of fit and experiment. We did not follow up this further, since only the 1642 and 1631 cm⁻¹ bands are important for this discussion.

We further investigated whether the fit result depends on replacing the broad baseline band at 1600 cm⁻¹ by a straight line or by two additional bands as in the previous work²⁰, or by the use of pure Gaussian lines²⁰. In particular baseline correction by a straight line increased the band area of the 1631 cm⁻¹ band to 12.2%. However, the second derivative of the fits deviates in the 1645 to 1635 cm⁻¹ region from the experimental second derivative indicating that the band widths are not correct.

In case of the work by Echabe et al.²⁵ there is a discrepancy between the band areas stated in their table 1 and the component bands plotted in their Fig. 1a. Reevaluation of this figure by filling the component bands with colour and counting the respective pixels with IrfanView gives a value of 12.5 % for the band near 1630 cm⁻¹ which is in excellent agreement with the value obtained with our baseline corrected spectrum. We conclude that our absorption spectrum allows fits that have comparable 1631 cm⁻¹ band areas as in previous work, but that the second derivative of such fits deviates from the experimental second derivative.

Subsequently, information from the IR spectrum and the X-ray structure were compared in order to assign the 1642 cm⁻¹ band. The crystal structure of the Ca₂E1 state of SERCA1a (pdb entry 1SU4)¹⁴ contains around 47% helical structure and 16% beta sheet determined by the DSSP algorithm⁵⁰ as implemented on *The Secondary Structure Server* (<http://2struc.cryst.bbk.ac.uk/twostruc>)⁵¹. In the IR spectrum, the band at 1632 cm⁻¹ is located in a region of β -sheet absorption. However, highly α -helical proteins without β -sheets also exhibit a side band close to 1630 cm⁻¹.^{42, 52-54} Therefore, only a part of this band can be assigned to β -sheets. The relative band area of this band is 4% of the total amide I band area. This is much smaller than the 16% contribution of β -sheets to the secondary structure and therefore other bands need to be assigned to β -sheets too. The only other possible β -sheet band is the band at 1642 cm⁻¹. Together with a fraction of the band at 1632 cm⁻¹ (0 - 4%) and of the high wavenumber component at 1691 cm⁻¹ (0 - 3%, typically less than 10% of the low wavenumber band area)⁵⁵, the band area assigned to β -sheet absorption contributes to 19 - 26% of the total amide I intensity, which is only slightly higher than the β -sheet content in the crystal structure. From this discussion we conclude that the 1642 cm⁻¹ band in the SERCA1a spectrum arises from β -sheet structure.

Table 1 Curve fitting analysis of a freshly prepared and of a 10 days old SERCA1a sample (stored at room temperature). In addition to the listed bands, the fit model contained a broad band at 1600 cm⁻¹, a small band at 1619 cm⁻¹ (fresh sample) or 1615 cm⁻¹ (aged sample) and a band at 1738 cm⁻¹ (fresh sample) or bands at 1732 and 1745 cm⁻¹ (aged sample). These are outside the amide I region and were not included in the analysis.

Wavenumber (cm ⁻¹)								
fresh sample	1631	1642	1655		1664*	1673*	1682	1691
10 days old sample	1632	1643	1654	1657*		1679		1694
Area (%)								
fresh sample	4	19	59		9	4	2	3
10 days old sample	11	12	23	33		21		<1

Assignment	α and β	β	α and unordered	turn	turn	turn	β and turns
------------	----------------------	---------	---------------------------	------	------	------	----------------------

*: Additional bands, not obvious in the second derivative spectra, were used to get the best fit in both absorption spectrum and second derivative analysis.

3.3 Washing with water and long-term storage decrease the 1642 cm^{-1} band and increase the 1631 cm^{-1} band

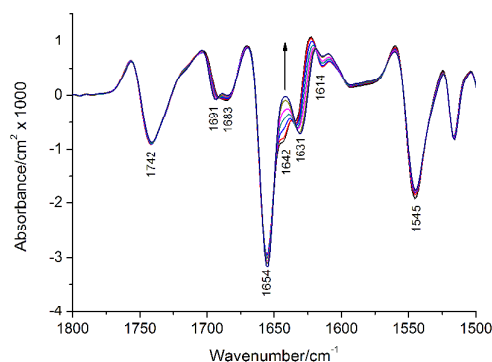


Fig. 3 Structural changes of rabbit SERCA1a upon repeated washing. Shown are second derivatives of ATR IR spectra after a series of ddH₂O washes. The spectra were normalised at 1742 cm^{-1} . The spectra from bottom to top at 1642 cm^{-1} were obtained after 1-7 times of washing with ddH₂O. The arrow indicates the spectral change at 1642 cm^{-1} upon repeated washing.

The following experiments were intended to destabilise SERCA1a by removal of Ca^{2+} and K^{+} ions and by extended storage at room temperature (20°C). Removal of Ca^{2+} inactivates the enzyme. This is most rapid for solubilised ATPase⁵⁶⁻⁵⁹ but has also been observed for membraneous ATPase⁵⁷. Our initial observation was that SERCA1a underwent a relatively large structural change when a protein film on the ATR crystal was washed with ddH₂O by adding water to the film, incubating for 5 min, and finally removing the liquid with tissue. The corresponding second derivative spectra are shown in Fig. 3. Upon repeated washing, most of the protein bands did not shift, except that the shoulder at 1642 cm^{-1} disappeared whereas the band at 1632 cm^{-1} shifted slightly downwards and became more dominant. These changes were irreversible and not observed upon washing with buffer (10 mM MOPS-KOH, 10 mM KCl, 20 μM CaCl_2 , pH 7.0). Protein aggregation is a possible explanation for these irreversible changes.

The same structural change in the infrared region was observed upon ageing. The sample was washed and then stored in Ca^{2+} free MOPS buffer (10 mM MOPS-KOH, 10 mM KCl, pH 7.0) at room temperature for several days. Fig. 4A shows the corresponding second derivative spectra. The spectrum of the 10 days old sample was fitted as described above for the fresh sample and the band areas are listed in Table 1. The numbers indicate that the 1642 cm^{-1} band loses nearly 40% of its area and that 7% of the total amide I area are redistributed from the 1642 cm^{-1} band to the 1631 cm^{-1} band.

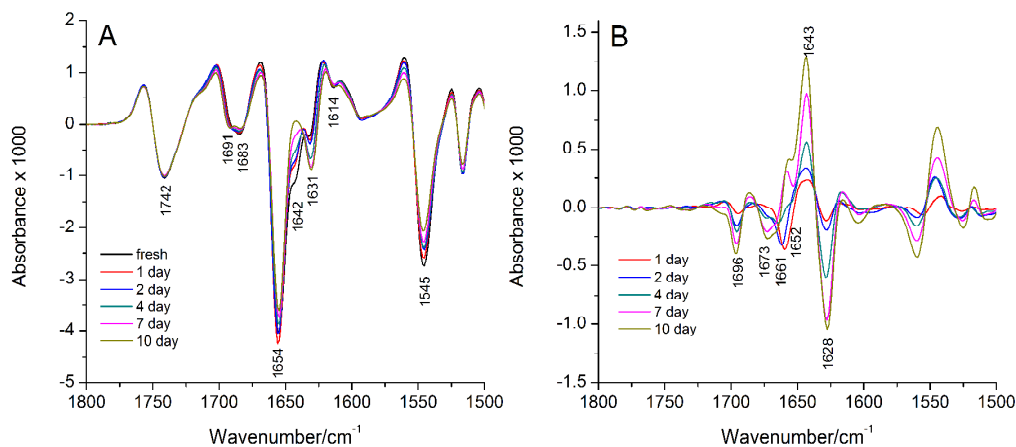


Fig. 4 Structural change of rabbit SERCA1a upon storage at room temperature in a Ca²⁺ free buffer. A: second derivatives of ATR IR absorption spectra of dried SERCA1a. The spectra were normalised at 1742 cm⁻¹ to the same lipid absorption; B: Subtraction of second derivative spectra: spectra of stored samples minus spectrum of a fresh sample.

For a more detailed analysis of the structural change upon storage, the second derivative spectrum from the freshly prepared SERCA1a sample was subtracted from the later spectra. The resulting second derivative difference spectra are shown in Fig. 4B. Negative bands in these spectra indicate increasing absorption and positive bands indicate decreasing absorption upon storage. Thus the main spectral feature is the shift from 1643 cm⁻¹ to 1628 cm⁻¹. This is associated with increased absorption at 1696 cm⁻¹ and an upshift of the amide II band. These bands are characteristic of β -sheet absorption. The main α -helix band at 1654 cm⁻¹ changes only little, which makes an assignment of the 1628 cm⁻¹ difference band to the low wavenumber component of α -helices unlikely. Therefore we attribute the main spectral changes to a structural change of β -sheets. Apart from this main process, other structural changes are reflected in the second derivative difference spectra, in particular in the early phase, where the spectral shape is different from that of the late spectra. The difference after day 1 and day 2 shows a prominent negative band at 1661 cm⁻¹, which is not observed in the late spectra, but no negative band at 1673 cm⁻¹, which is present in the late spectra.

3.4 Does the 1642 cm⁻¹ band correlate with activity?

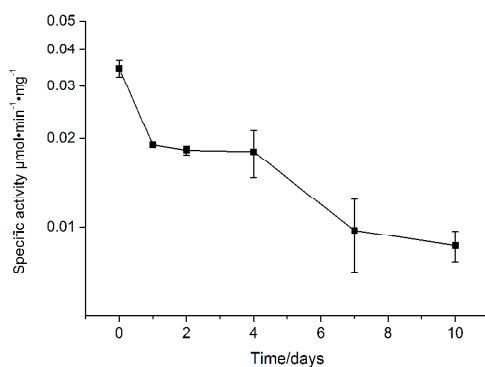


Fig. 5 Enzyme specific activity of SERCA1a at 1 °C after storage at room temperature for several days. Data from 3 flashes were averaged to give a mean value. The standard deviation of the activity in spectral units is also indicated. Conversion to SI units generates an additional error of 35% which is the same for all data points.

The activity of the ATPase after different times of storage was measured by reaction-induced difference IR spectroscopy as described in Materials and Methods. The results are shown in Fig. 5. The samples were stored at room temperature (20°C) without added Ca^{2+} in the buffer but the activity measurements were performed in the presence of Ca^{2+} and at 1°C. The initial activity is lower than in our previous work ($0.06 \mu\text{mol min}^{-1} \text{mg}^{-1}$)²⁸ likely because of the initial centrifugation step without Ca^{2+} . Within 10 days, the activity dropped to ~25% of its initial value. The activity drop was somewhat larger than observed for membraneous ATPase at saturating Ca^{2+} concentrations, comparable to that of DDM solubilised ATPase in the presence of Ca^{2+} , less than that of C_{12}E_8 solubilised ATPase in the presence of Ca^{2+} , and much less than for detergent solubilised ATPase in the absence of Ca^{2+} ^{58, 59}.

The main activity drop in our experiment was within one day, corresponding to 65% of the activity change over 10 days. This behaviour is not reflected in the difference second derivative spectra, where the changes after the first day are only 18%, 15%, and 16% of the total change for the 1628, 1643 and 1696 cm^{-1} bands, respectively. Subsequently, the changes increase linearly up to day 7. Therefore we conclude that the main activity decrease upon extended storage at room temperature precedes the structural change of the β -sheets. A further argument indicates that there is no simple correlation between the second derivative spectrum and the activity. The 1631 cm^{-1} band is slightly larger for the recombinant protein than for the aged protein after 10 days, when the spectra are normalised to the integrated absorbance in the amide I region. Thus the activity of the recombinant protein should be less than that of the 10 days aged protein, i.e. less than 20% of the activity of the rabbit protein. However, it is higher than expected on the basis of the spectra, i.e. about 50% of that of the rabbit protein.²⁸

3.5 Protein aggregation leads to a reduction of the 1642 cm^{-1} band

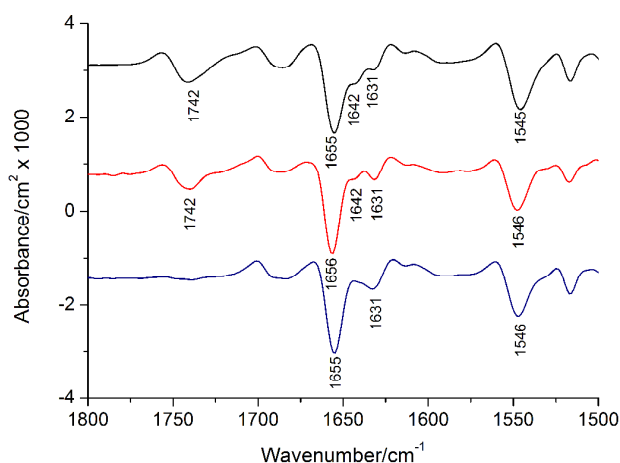


Fig. 6 Second derivative of rabbit SERCA1a absorption spectra before and after detergent solubilisation. Black: membrane bound SERCA1a; red: solubilised SERCA1a in $1 \text{ mg}\cdot\text{mL}^{-1}$ DDM; blue: insolubilised pellet.

To investigate whether the disappearing of the 1642 cm^{-1} band was caused by protein aggregation, rabbit SERCA1a was solubilised with detergent and centrifuged at 154000 g for 1 h. $1 \text{ mg}\cdot\text{mL}^{-1}$ DDM was chosen to solubilise protein because it does not have an IR absorption between 1800 and 1500 cm^{-1} and it does not cause a fundamental structural change of the solubilised SERCA1a^{60, 61}. Non-solubilised protein (aggregated or vesicles) was

1
2
3 removed by centrifugation. In case of incomplete solubilisation of the SR membrane,
4 remaining vesicles are expected to end up in the pellet because the centrifugation speed was
5 tested before to be sufficient to sediment the vesicles. However, there was no lipid band (1742
6 cm^{-1}) observed in the pellet spectrum (Fig. 6, blue spectrum) giving evidence for successful
7 solubilisation. Thus, solubilised protein together with solubilised lipid were found in the
8 supernatant as demonstrated by the supernatant spectrum (red spectrum in Fig. 6), which
9 contained the lipid band at 1740 cm^{-1} and protein bands in the amide I region. As shown in
10 Fig. 6, solubilised SERCA1a retained the structure of the membrane bound protein with a
11 clear band at 1642 cm^{-1} . The pellet (blue spectrum) contained aggregated protein, which had a
12 higher absorption at 1631 cm^{-1} , and no obvious shoulder at 1642 cm^{-1} . This indicates that
13 protein aggregates do not exhibit a clear band at 1642 cm^{-1} in their second derivative spectra
14 and instead show a prominent band at 1631 cm^{-1} .
15
16

17 4. Discussion

18
19 Although the recombinant protein resembles rabbit SERCA1a in terms of the conformational
20 changes associated with the formation of different enzyme intermediates in the reaction cycle,
21 it showed observable differences in the infrared absorption spectrum in the region around
22 1640 cm^{-1} . The recombinant protein had a dominant 1631 cm^{-1} band whereas the shoulder at
23 1642 cm^{-1} in the native protein sample was less obvious in the recombinant sample. We
24 consider it unlikely that these differences can be explained by the different impurities in the
25 two samples. First, the 1642 cm^{-1} band is also present in purified ATPase,^{18, 20, 21, 25} and
26 second, the rabbit spectrum can be converted into a spectrum that resembles that of the
27 recombinant ATPase by washing with water, storage at room temperature and aggregation
28 after solubilisation.
29
30

31 Although several IR studies have been conducted on the structure of SERCA1a, the band at
32 1642 cm^{-1} had not been clearly assigned. Relating the IR spectrum to 3D structural
33 information, we assigned this band to β -sheet structure. β -sheet bands shift to lower
34 wavenumber when the number of strands in the sheet increases and to higher wavenumber
35 when the sheet is distorted.^{62, 63} The relatively high wavenumber of the band indicates
36 therefore distorted or twisted sheets.
37

38 The spectral differences between rabbit and recombinant SERCA1a are similar to
39 absorbance changes of rabbit SERCA1a upon ageing at room temperature and upon washing
40 with water, which are associated with a decrease in the 1642 cm^{-1} band and an increase of a
41 band at 1631 cm^{-1} . These changes resemble those of $\text{Ca}_2\text{E1P}$ formation from $\text{Ca}_2\text{E1}$ in the β -
42 sheet region,^{24, 34} which we have tentatively assigned to the β -sheet in the P domain that
43 becomes more flat upon nucleotide binding and phosphorylation. A similar flattening of β -
44 sheets and/or an increase in the number of strands by intermolecular contacts could also be an
45 explanation for the changes seen upon ageing and washing. However, the changes observed
46 upon ageing and washing are about 10-fold larger than those observed in the ATPase reaction
47 cycle. They seem to involve 30-40% of the β -sheets absorbing at 1642 cm^{-1} as judged from
48 the difference in relative band areas between aged and fresh sample (Table 1). The observed
49 structural changes are located in the cytoplasmic domains, since the transmembrane domain
50 does not contain β -sheets.
51

52 Apart from washed, aged and recombinant SERCA1a, also ATPase that aggregated upon
53 solubilisation shows a prominent band near 1631 cm^{-1} . This could indicate that a fraction of
54 the recombinant enzyme forms aggregates, which would explain its 50% lower specific
55 activity as compared to the preparation from rabbit muscle. However, there were also some
56 clear differences between the recombinant and the protein aggregates that form upon
57 solubilisation: (i) the aggregated protein after solubilisation shows a shoulder on the high
58
59
60

1
2
3 wavenumber side of the 1631 cm^{-1} band, which is not present in the spectrum of the
4 recombinant ATPase and which has a lower band position than the 1642 cm^{-1} band of the
5 solubilised and the membranous rabbit ATPase, (ii) the 1631 cm^{-1} band is less prominent for
6 the aggregated protein than for the recombinant protein, and (iii) the pellet of the aggregated
7 protein could not be dissolved in buffer, whereas this was not a problem for the recombinant
8 ATPase. These differences indicate that the structures of recombinant and aggregated ATPase
9 were different and that larger or more stable aggregates exist in the pellet after solubilisation.
10 The modified β -sheet structures in the recombinant preparation can be dissolved in SDS as
11 there is no indication for a substantial fraction of aggregates in our preparation from gel
12 electrophoresis.²⁸

14 While the band near 1631 cm^{-1} seems to indicate aggregation, it is not a direct measure of
15 enzyme activity. This conclusion is supported by two arguments: (i) The formation of the
16 1631 cm^{-1} band upon aging has a different time course than the loss of activity. (ii) The
17 amplitude of the 1631 cm^{-1} band is larger for recombinant SERCA1a than for the aggregates
18 formed upon solubilisation. The latter are known to be inactive,^{59, 64} whereas recombinant
19 ATPase retains 50% of the activity of the rabbit enzyme. Thus, the recombinant protein has
20 higher activity although the 1631 cm^{-1} band indicates a larger impact of recombinant protein
21 production on the structure of the β -sheets. It is possible that protein-protein associations in
22 the membrane environment of the recombinant ATPase mainly proceed via contacts between
23 the cytosolic domains and cause relative large structural changes in their β -sheets, whereas
24 solubilisation enables protein-protein interaction also in the α -helical transmembrane region,
25 which could generate different aggregates with relatively little perturbation of the cytosolic β -
26 sheets.

28 The 1631 cm^{-1} band of aged, washed, and aggregated rabbit SERCA1a and of recombinant
29 SERCA1a has a similar position as a prominent β -sheet band found between 1630 and 1625
30 cm^{-1} in inclusion bodies^{6, 7, 9}. For interleukin 1β and the green fluorescent protein, the increase
31 of the band near 1630 cm^{-1} upon formation of inclusion bodies is associated with a reduction
32 of a band near 1640 cm^{-1} .^{6, 9} In case of interleukin 1β this reduction has been quantified: it
33 corresponds to 50% of the band area of the native protein, which is very similar to what is
34 observed here for SERCA1a upon ageing. The $\sim 1630\text{ cm}^{-1}$ band of aggregates reveals that
35 their structure differs for different treatments. For human growth hormone and human
36 interferon-alpha-2b, the aggregate band absorbs at the highest wavenumber when the
37 inclusion bodies are produced by a low producing strain, it is downshifted by a few cm^{-1} for a
38 higher producing strain and absorbs at even lower wavenumber when the aggregates are
39 generated by high temperature.⁷

42 Finally, we turn the focus to the properties of the active fraction of recombinant ATPase,
43 which for our preparation amounts to $\sim 50\%$ of that of the rabbit muscle preparation. We have
44 previously shown that it undergoes the same conformational changes as the rabbit enzyme.²⁸
45 Furthermore, recombinant SERCA1a was able to crystallise in octaethylene glycol
46 monododecyl ether (C_{12}E_8) in the presence of excess 1,2-dioleoyl-*sn*-glycero-3-
47 phosphocholine (DOPC) and the wild type enzyme structure was found to be
48 indistinguishable from that of the native rabbit enzyme.³⁰ Some mutants of SERCA1a
49 crystallised as well without hints of specific β -sheet modifications.^{65, 66} The crystals were
50 grown after an additional size exclusion chromatography step which was followed by
51 centrifugation, which is likely to remove most of the aggregated protein. Thus, the available
52 structural and dynamical data all indicate that the active fraction of recombinant SERCA1a
53 closely corresponds to the rabbit enzyme.

5. Conclusion

We conclude that ageing and washing of rabbit SERCA1a as well as the recombinant production of SERCA1a leads to β -sheet structures that are similar to those of aggregated SERCA1a and of inclusion bodies from other proteins. A reasonable molecular interpretation of the spectra is that these β -sheets are more planar and/or contain more strands than those of the fresh rabbit enzyme and comprise about half of its β - sheets. The active fraction of recombinant SERCA1a on the other hand behaves in all aspects studied so far like the enzyme prepared from rabbit muscle.

Our finding of spectral markers for aggregation will be beneficial for the optimisation of the production of recombinant proteins, since it provides a convenient way to check the structure of the protein product and to assess its integrity and stability under various conditions, including those used in crystallisation trials. In using IR spectroscopy for quality control of recombinant proteins, it is beneficial that the method can focus on the active fraction only, as in our previous work,²⁸ or on the total protein pool as used here. In this way it is possible to characterise both the active and inactive protein fractions.

Acknowledgements

The authors thank W. Hasselbach (Max-Planck-Institut, Heidelberg, Germany) for the gift of Ca^{2+} -ATPase and J.E.T. Corrie for the caged ATP. This work was supported by Knut och Alice Wallenbergs Stiftelse.

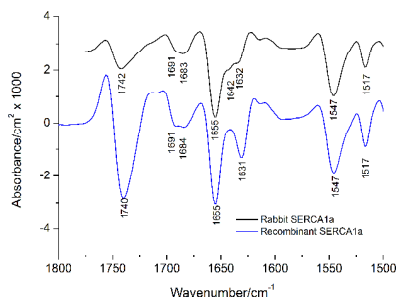
Notes and references

1. A. Elliott and E. J. Ambrose, *Nature*, 1950, **165**, 921-922.
2. M. Jackson and H. H. Mantsch, *Critical reviews in biochemistry and molecular biology*, 1995, **30**, 95-120.
3. A. Barth, *Biochimica et biophysica acta*, 2007, **1767**, 1073-1101.
4. J. Kong and S. Yu, *Acta biochimica et biophysica Sinica*, 2007, **39**, 549-559.
5. S. Ventura and A. Villaverde, *Trends in biotechnology*, 2006, **24**, 179-185.
6. M. Martinez-Alonso, N. Gonzalez-Montalban, E. Garcia-Fruitos and A. Villaverde, *Applied and environmental microbiology*, 2008, **74**, 7431-7433.
7. D. Ami, A. Natalello, G. Taylor, G. Tonon and S. M. Doglia, *Biochimica et biophysica acta*, 2006, **1764**, 793-799.
8. A. A. Valdivia, A. Barth, Y. R. Batista and S. Kumar, *Biologicals : journal of the International Association of Biological Standardization*, 2013, **41**, 104-110.
9. K. Oberg, B. A. Chrnyk, R. Wetzels and A. L. Fink, *Biochemistry*, 1994, **33**, 2628-2634.
10. S. Seshadri, R. Khurana and A. L. Fink, *Methods in enzymology*, 1999, **309**, 559-576.
11. W. Hasselbach and M. Makinose, *Biochemische Zeitschrift*, 1961, **333**, 518-528.
12. L. de Meis and A. L. Vianna, *Annual review of biochemistry*, 1979, **48**, 275-292.
13. J. V. Møller, P. Nissen, T. L. Sørensen and M. le Maire, *Current opinion in structural biology*, 2005, **15**, 387-393.
14. C. Toyoshima, M. Nakasako, H. Nomura and H. Ogawa, *Nature*, 2000, **405**, 647-655.

- 1
 - 2
 - 3
 - 4
 - 5
 - 6
 - 7
 - 8
 - 9
 - 10
 - 11
 - 12
 - 13
 - 14
 - 15
 - 16
 - 17
 - 18
 - 19
 - 20
 - 21
 - 22
 - 23
 - 24
 - 25
 - 26
 - 27
 - 28
 - 29
 - 30
 - 31
 - 32
 - 33
 - 34
 - 35
 - 36
 - 37
 - 38
 - 39
 - 40
 - 41
 - 42
 - 43
 - 44
 - 45
 - 46
 - 47
 - 48
 - 49
 - 50
 - 51
 - 52
 - 53
 - 54
 - 55
 - 56
 - 57
 - 58
 - 59
 - 60
15. C. Toyoshima and H. Nomura, *Nature*, 2002, **418**, 605-611.
16. T. L. Sørensen, J. V. Møller and P. Nissen, *Science*, 2004, **304**, 1672-1675.
17. C. Toyoshima, S. Iwasawa, H. Ogawa, A. Hirata, J. Tsueda and G. Inesi, *Nature*, 2013, **495**, 260-264.
18. D. C. Lee, J. A. Hayward, C. J. Restall and D. Chapman, *Biochemistry*, 1985, **24**, 4364-4373.
19. R. Mendelsohn, G. Anderle, M. Jaworsky, H. H. Mantsch and R. A. Dluhy, *Biochimica et biophysica acta*, 1984, **775**, 215-224.
20. J. Villalain, J. C. Gomez-Fernandez, M. Jackson and D. Chapman, *Biochimica et biophysica acta*, 1989, **978**, 305-312.
21. J. A. Teruel, J. Villalain and J. C. Gomez-Fernandez, *The International journal of biochemistry*, 1990, **22**, 779-783.
22. R. Buchet, S. Varga, N. W. Seidler, E. Molnar and A. Martonosi, *Biochimica et biophysica acta*, 1991, **1068**, 201-216.
23. A. Troullier, K. Gerwert and Y. Dupont, *Biophysical journal*, 1996, **71**, 2970-2983.
24. A. Barth, F. von Germar, W. Kreutz and W. Mäntele, *The Journal of biological chemistry*, 1996, **271**, 30637-30646.
25. I. Echabe, U. Dornberger, A. Prado, F. M. Goni and J. L. Arrondo, *Protein science : a publication of the Protein Society*, 1998, **7**, 1172-1179.
26. A. Barth, W. Kreutz and W. Mäntele, *FEBS letters*, 1990, **277**, 147-150.
27. B. Ma, C. J. Tsai, T. Haliloglu and R. Nussinov, *Structure*, 2011, **19**, 907-917.
28. S. Kumar, C. Li, C. Montigny, M. le Maire and A. Barth, *The FEBS journal*, 2013, **280**, 5398-5407.
29. L. De Meis and W. Hasselbach, *The Journal of biological chemistry*, 1971, **246**, 4759-4763.
30. M. Jidenko, R. C. Nielsen, T. L.-M. Sørensen, J. V. Møller, M. le Maire, P. Nissen and C. Jaxel, *Proceedings of the National Academy of Sciences of the United States of America*, 2005, **102**, 11687-11691.
31. M. Jidenko, G. Lenoir, J. M. Fuentes, M. le Maire and C. Jaxel, *Protein expression and purification*, 2006, **48**, 32-42.
32. D. Cardi, C. Montigny, B. Arnou, M. Jidenko, E. Marchal, M. le Maire and C. Jaxel, *Methods in molecular biology*, 2010, **601**, 247-267.
33. A. Barth, W. Kreutz and W. Mäntele, *Biochimica et biophysica acta*, 1994, **1194**, 75-91.
34. H. Georg, A. Barth, W. Kreutz, F. Siebert and W. Mäntele, *Biochimica et biophysica acta*, 1994, **1188**, 139-150.
35. A. Barth, W. Mäntele and W. Kreutz, *Biochimica et biophysica acta*, 1991, **1057**, 115-123.
36. D. Thoenges and A. Barth, *Journal of biomolecular screening*, 2002, **7**, 353-357.
37. H. Takeuchi, H. Murata and I. Harada, *Journal of the American Chemical Society*, 1988, **110**, 392-397.
38. A. Barth, *PhD Thesis, Albert-Ludwigs-Universität Freiburg, Germany*, 1992.
39. B. de Foresta, M. le Maire, S. Orłowski, P. Champeil, S. Lund, J. V. Møller, F. Michelangeli and A. G. Lee, *Biochemistry*, 1989, **28**, 2558-2567.
40. J. L. Arrondo, H. H. Mantsch, N. Mullner, S. Pikula and A. Martonosi, *The Journal of biological chemistry*, 1987, **262**, 9037-9043.
41. A. Barth, *Spectrochimica acta. Part A, Molecular and biomolecular spectroscopy*, 2000, **56**, 1223-1232.
42. D. M. Byler and H. Susi, *Biopolymers*, 1986, **25**, 469-487.
43. F. Dousseau and M. Pezolet, *Biochemistry*, 1990, **29**, 8771-8779.

- 1
2
3 44. D. C. Lee, P. I. Haris, D. Chapman and R. C. Mitchell, *Biochemistry*, 1990, **29**, 9185-
4 9193.
5 45. R. W. Sarver, Jr. and W. C. Krueger, *Analytical biochemistry*, 1991, **194**, 89-100.
6 46. T. Heimburg, J. Schuenemann, K. Weber and N. Geisler, *Biochemistry*, 1996, **35**,
7 1375-1382.
8 47. B. I. Baello, P. Pancoska and T. A. Keiderling, *Analytical biochemistry*, 2000, **280**,
9 46-57.
10 48. J. A. Hering, P. R. Innocent and P. I. Haris, *Proteomics*, 2002, **2**, 839-849.
11 49. J. Ollesch, E. Kunnemann, R. Glockshuber and K. Gerwert, *Applied spectroscopy*,
12 2007, **61**, 1025-1031.
13 50. W. Kabsch and C. Sander, *Biopolymers*, 1983, **22**, 2577-2637.
14 51. D. P. Klose, B. A. Wallace and R. W. Janes, *Bioinformatics*, 2010, **26**, 2624-2625.
15 52. P. I. Haris and F. Severcan, *Journal of Molecular Catalysis B: Enzymatic*, 1999, **7**,
16 207-221.
17 53. D. C. Lee, E. Herzyk and D. Chapman, *Biochemistry*, 1987, **26**, 5775-5783.
18 54. P. I. Haris, M. Coke and D. Chapman, *Biochimica et biophysica acta*, 1989, **995**, 160-
19 167.
20 55. S. Venyaminov and N. N. Kalnin, *Biopolymers*, 1990, **30**, 1259-1271.
21 56. N. Ikemoto, G. M. Bhatnager and J. Gergely, *Biochem. Biophys. Res. Commun.*, 1971,
22 **44**, 1510-1517.
23 57. B. Vilsen and J. P. Andersen, *European journal of biochemistry / FEBS*, 1987, **170**,
24 421-429.
25 58. C. Montigny, B. Arnou and P. Champeil, *Biochemical and biophysical research*
26 *communications*, 2010, **391**, 1067-1069.
27 59. P. Champeil, T. Menguy, C. Tribet, J.-L. Popot and M. le Maire, *Journal of Biological*
28 *Chemistry*, 2000, **275**, 18623-18637.
29 60. W. Welte, M. Leonhard, K. Diederichs, H. U. Weltzien, C. Restall, C. Hall and D.
30 Chapman, *Biochimica et biophysica acta*, 1989, **984**, 193-199.
31 61. M. le Maire, P. Champeil and J. V. Møller, *Biochimica et biophysica acta*, 2000, **1508**,
32 86-111.
33 62. Y. N. Chirgadze and N. A. Nevskaya, *Biopolymers*, 1976, **15**, 627-636.
34 63. J. Kubelka and T. A. Keiderling, *J. Am. Chem. Soc.*, 2001, **123**, 12048-12058.
35 64. J. P. Andersen, B. Vilsen, H. Nielsen and J. V. Møller, *Biochemistry*, 1986, **25**, 6439-
36 6447.
37 65. A. Marchand, A. M. Winther, P. J. Holm, C. Olesen, C. Montigny, B. Arnou, P.
38 Champeil, J. D. Clausen, B. Vilsen, J. P. Andersen, P. Nissen, C. Jaxel, J. V. Møller
39 and M. le Maire, *The Journal of biological chemistry*, 2008, **283**, 14867-14882.
40 66. J. D. Clausen, M. Bublitz, B. Arnou, C. Montigny, C. Jaxel, J. V. Møller, P. Nissen, J.
41 P. Andersen and M. le Maire, *The EMBO journal*, 2013, **32**, 3231-3243.
42
43
44
45
46
47
48
49
50
51
52
53
54
55
56
57
58
59
60

Table of contents entry



FTIR spectroscopy detects aggregates of recombinantly produced protein and can therefore be used for quality control.